The analytical and numerical study of alternative fuel injectors for the purpose of reducing chemical pollution in aviation sector

Grigore CICAN*,[1], Georgiana Cristina ICHIM[1]

*Corresponding author
[1]Department of Aerospace Sciences, POLITEHNICA University Bucharest,
Splaiul Independentei 313, 060042, Bucharest, Romania,
grigore.cican@upb.ro*

DOI: 10.13111/2066-8201.2023.15.4.7

Received: 23 October 2023/ Accepted: 07 November 2023/ Published: December 2023

Abstract: *In this paper, both analytical and numerical analyses are conducted to study the behavior of a simplex time injector with a swirl chamber represented by a pin, designed to operate with kerosene. In an effort to reduce chemical pollution, the injector's performance when operating with alternative fuels such as biofuel and ethanol is investigated. Calculations have been performed to analyze the use of these three fuels at various pressures up to 100 bar. Analytical calculations were used to determine parameters such as spray angle, droplet size, fuel film thickness, and more. For a better visualization of the phenomena occurring during the injector's operation with these three fuels, numerical simulations were carried out using ANSYS, and the spray of droplets at various pressures at the injector inlet was presented. The study revealed that among the liquids studied, ethanol is the most optimal fuel. Ethanol has low viscosity and low density, making it easier to atomize by our injector compared to pure biofuel, which has higher density and viscosity values. The calculations demonstrated the qualities of ethanol following atomization, including a thin liquid film, a wide spray angle consisting of small-sized droplets, at any pressure difference, compared to the other studied fuels. It was observed that pressure difference has a significant impact on the atomization of a liquid. The best atomization qualities and optimal values were achieved when the pressure difference is high.*

Key Words: *alternative fuel, injector, numerical simulations, analytical calculus, atomization, spray angle*

1. INTRODUCTION

Especially in the aviation and aerospace industries, a series of intricate chemical and physical transformations occur during combustion processes, leading to the inevitable production of pollutants. It has been noted that the interactions among various emitted pollutants are significantly influenced by fuel properties like fuel density, viscosity, and surface tension [1]. In an effort to improve atomization quality and reduce pollutant emissions, engineers are looking to modify fuel properties by combining conventional fuels with renewable fuels, such as biofuel used in piston engines [2] or turbo engines [3, 4, 5], alcohols for piston engines [6, 7, 8] or turbo engines [9, 10]. Typically, spray quality is primarily characterized by spray cone angle, discharge coefficient, and breakup length. Initially, the spray cone angle and spray velocity of the pressure-swirl nozzle impact fuel combustion and pollutant emissions. A

reduction in spray cone angle is advantageous for improving combustion efficiency at low power conditions. However, a larger spray cone angle and higher spray velocity result in enhanced gas-fuel mixing and wider fuel coverage. Additionally, it has been observed that these factors are influenced by liquid properties [11]. Increased dispersion leads to lower fuel concentrations, resulting in reduced emissions and diminished soot formation. Thus, the spray cone angle plays a pivotal role in determining spray characteristics and ultimately affects ignition success [12]. Song et al. [13] conducted experimental research on the spray characteristics of ethanol-kerosene blended fuels and noted that ethanol addition has a certain effect on spray characteristics. However, the results suggested that a 20% ethanol blend in kerosene does not significantly impact spray performance compared to kerosene. Their study primarily focused on the spray characteristics of a direct jet nozzle, making their conclusions less applicable to the pressure-swirl nozzle. In [14], spray characteristics of kerosene-based fuel (Jet A-1) and alternative aviation fuels, such as butyl butyrate, butanol, and their blends with Jet A-1, were investigated using an airblast atomizer under various atomizing air-to-fuel ratios. The aim was to understand how changes in fuel properties (particularly viscosity) influence atomization. Due to the higher viscosity of butanol, the Sauter Mean Diameter (SMD) is higher, and droplet formation appears to be delayed compared to Jet A-1. In contrast, the lower viscosity of butyl butyrate promotes faster droplet formation. The effects of blending these biofuels with Jet A-1 on atomization characteristics were also compared with Jet A-1 alone. Currently, biofuels with properties similar to Jet A-1 hold promise as alternative aviation fuels to address fuel-related challenges [15].

In this paper, both analytical and numerical analyses are performed to investigate the performance of a simplex time injector with a swirl chamber represented by a pin, designed for kerosene operation. In an effort to reduce chemical pollution, the study explores the injector performance when operating with alternative fuels such as biofuel and ethanol.

2. MATERIALS AND METHODS

In principle, atomization is the process in which the volume of liquid breaks down into fine droplets, under the action of internal and external forces. The fine and thin spraying of the fuel is achieved in two stages: primary atomization and secondary atomization. In the primary atomization stage, the droplets are obtained by breaking down the jet or a sheet of liquid, while secondary atomization is used to obtain smaller-sized droplets and occurs when the droplets formed in the first atomization stage come into contact with the ambient flow. One of the methods of fuel atomization is to introduce it into the swirl chamber through tangentially arranged slots, providing the fuel with turbulent motion. This motion represents a decrease in fuel pressure, resulting in the formation of a vortex inside the swirl chamber. Subsequently, the swirled fuel passes through the discharge orifice into the combustion chamber, where, based on its atomization, the turbulent motion is eliminated, forming a conical spray. The shape of the jet indicates the degree of fuel atomization [16].

2.1 Injector characteristics and fuels properties

Within the mathematical model, we will study the characteristics of the spray from a Simplex-type injector, considered the simplest atomizer model. This Simplex injector model is chosen because it includes a pin that ensures the rotational movement of the fuel. More specifically, a Simplex-type injector with axial helical slots will be used. The injector geometry has been selected in accordance with the source[17]. Figure 1a depicts the 3D image of the selected injector, while the representation of the pin responsible for the rotational motion aimed at fuel

atomization is shown in Figure 1b). The four intake swirl orifices, through which the fuel passes when the pin is in motion, can be observed.

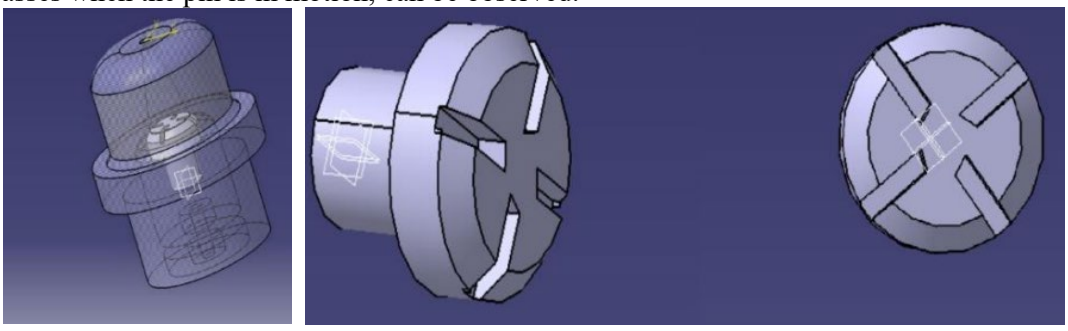

a) b)

Figure 1. 3D Injector and the pin

For a better visualization of the injector and its dimensions, Figure 2 provides a 2D representation of the injector used in the calculations. The direction of fuel flow inside the injector is indicated by arrows. Dimensions are expressed in millimeters (mm).

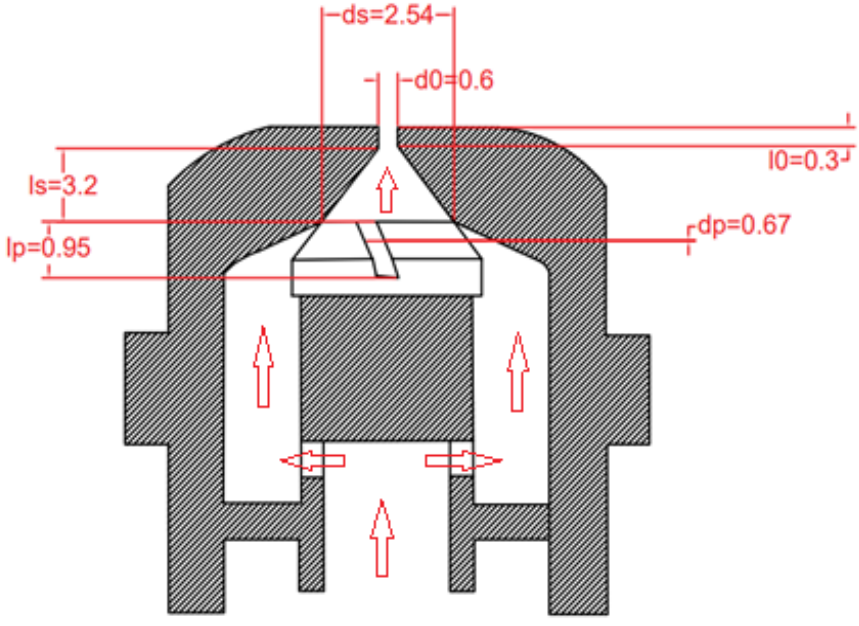

Figure 2. 2D injector representation

We will use three fuels (kerosene, ethanol, and pure biofuel) to observe the properties each aviation fuel has. After this analysis, we will determine which fuel is more optimal for the chosen injector. The quality characteristics of the studied fuels are presented in Table 1.

Table 1. Fuels properties [18]

Fuel	Dynamic viscosity kg/(m*s)	Density kg/m^3
Kerosene	$1.845 \cdot 10^{-3}$	802
Biofuel	$4.654 \cdot 10^{-3}$	895
Ethanol	$7.101 \cdot 10^{-4}$	789

2.2 Analytical model

Calculations are performed to determine the discharge coefficient, the flow number, the spray angle, the average droplet size of the atomized liquid, the velocity, and the Ohnesorge number. These characteristics of the fuel film are calculated based on the variation of the pressure difference.

Different values of the pressure difference (the difference between the outlet pressure and the inlet pressure in the injector) will be used to observe its influence on liquid atomization. Ten values of the pressure difference are selected, with the smallest value being 1 MPa and the largest value equal to 10 MPa. Surface tension is assumed to be the same for all fuels, with close values that do not significantly affect the calculated values. The formulas used for calculating the coefficients that determine the proper atomization of the fuel are presented below. The discharge coefficient is calculated using the formula:

$$\dot{m}_L = C_D A_0 (2\rho_L \Delta P_L)^{0,5} \text{ [kg/s]} \tag{1}$$

Implies that C_D:

$$C_D = \frac{m_L}{A_0\sqrt{2\rho_L \Delta P}} \tag{2}$$

The effective flow area is represented by the flow rate number. Thus, the flow rate number is calculated using the formula:

$$FN = \frac{m_L}{\sqrt{\Delta P \rho_L}} \ [m^2] \tag{3}$$

Film thickness is defined as:

$$t = 2{,}7\left(\frac{d_0 FN_L \mu_L}{\sqrt{\Delta P \rho_L}}\right)^{0,25} \ [m] \tag{4}$$

The spray angle for fuel is calculated using the formula:

$$2\theta = 6\left(\frac{d_s d_0}{A_p}\right)^{0,15} \cdot \left(\frac{\Delta P {d_0}^2 \rho_L}{{\mu_L}^2}\right)^{0,11} \ [^\circ] \tag{5}$$

The average droplet size (Sauter mean size) is calculated

$$SMD = 4{,}52\left(\sigma\frac{\mu_L^2}{\rho_a \Delta P^2}\right)^{0,25}(t\cos\theta)^{0,25} + 0{,}39\left(\sigma\frac{\rho_L}{\rho_a \Delta P}\right)^{0,25}(t\cos\theta)^{0,75} \ [mm] \tag{6}$$

Velocity is calculated using the formula:

$$U = \sqrt{\frac{2\Delta P}{\rho_L}} \ [m/s] \tag{7}$$

The Ohnesorge number for fuel is calculated

$$Z = \frac{\mu_L}{\sqrt{\rho_L \sigma d_0}} \tag{8}$$

The Weber number is calculated

$$We = \frac{\rho_A U^2 D}{\sigma} \tag{9}$$

2.3 Numerical simulations

In this work, specialized software will be used to provide accurate simulations of the atomization of kerosene, ethanol, and biofuel through the proposed injector. Ansys Fluent is a software that offers a range of tools for designing and optimizing new equipment. It provides insights into the real-life behavior of equipment that will be installed in aircraft engines and other fields. This software will help us better understand how fuel is atomized through a swirl chamber atomizer. Ansys Fluent offers high precision, and the results obtained from simulating the flow of kerosene, ethanol, and biofuel will be compared with the results obtained from calculations. With the help of this software, we will analyze the quality of atomization that the fuel exhibits when different pressure difference values are applied. Three simulations will be conducted specifically for $\Delta P = 1.00E + 06$ Pa, $\Delta P = 5.00E + 06$ Pa, and $\Delta P = 1.00E + 07$ Pa. The geometry used to simulate the atomization of kerosene, ethanol, and biofuel has been created. It consists of a simplex-type injector with a swirl chamber that atomizes the liquid inside a combustion chamber. Figure 3 illustrates the geometry used for the simulation. In this figure, the walls of the combustion chamber are represented transparently to better visualize the positioning of the injector.

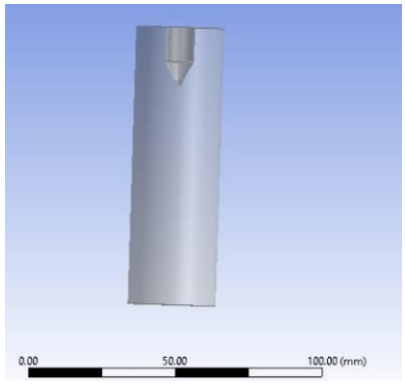

Figure 3. Representation of the geometry used for simulation

In the following figures, the initial conditions for numerical simulation are presented.

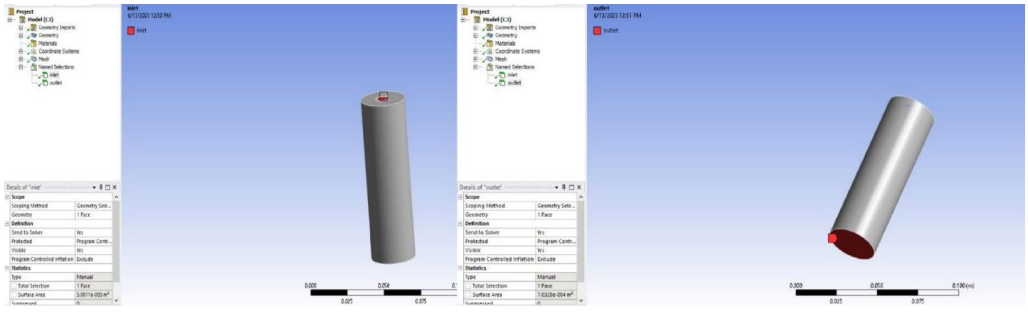

Figure 4. Presentation of initial conditions

A total of 17,173 nodes were created on the study surface, along with 86,980 elements. For the simulations, a number of time steps were defined as 5,000, with a time step size of 5E-6 [s], and a maximum number of iterations per time step set to 10. In the simulation, half of the spray angle is imposed, using half of the spray angle obtained for kerosene in the calculations. The fluid temperature is set to 300 K.

3. RESULTS AND DISCUSSIONS

The results were obtained for a fuel flow rate of 0.068 kg/s, with air density assumed at sea level, 1.225 kg/m^3, gravitational acceleration g=9.807 m/s^2, and surface tension sigma=0.0263257 N/m.

3.1 Analytical results

Fuel	Pressure [MPa]									
	1	2	3	4	5	6	7	8	9	10
Discharge coefficient CD										
Kerosene	0.601	0.425	0.347	0.300	0.269	0.245	0.227	0.212	0.200	0.190
Biofuel	0.568	0.402	0.328	0.284	0.254	0.232	0.215	0.201	0.190	0.180
Ethanol	0.605	0.428	0.350	0.303	0.271	0.247	0.229	0.214	0.202	0.192
Flow rate number FN [m^2]										
Kerosene	2.4E-07	1.7E-07	1.4E-07	1.2E-07	1.1E-07	9.8E-08	9.1E-08	8.5E-08	8.0E-08	7.6E-08
Biofuel	2.27E-07	1.61E-07	1.31E-07	1.14E-07	1.02E-07	9.28E-08	8.59E-08	8.04E-08	7.58E-08	7.19E-08
Ethanol	2.42E-07	1.71E-07	1.40E-07	1.21E-07	1.08E-07	9.88E-08	9.15E-08	8.56E-08	8.07E-08	7.66E-08
Film thickness t [m]										
Kerosene	1.49E-04	1.26E-04	1.14E-04	1.06E-04	9.99E-05	9.55E-05	9.19E-05	8.89E-05	8.63E-05	8.40E-05
Biofuel	1.83E-04	1.54E-04	1.39E-04	1.30E-04	1.23E-04	1.17E-04	1.13E-04	1.09E-04	1.06E-04	1.03E-04
Ethanol	1.18E-04	9.94E-05	8.98E-05	8.36E-05	7.90E-05	7.55E-05	7.27E-05	7.03E-05	6.82E-05	6.65E-05
Spray nozzle angle[°]										
Kerosene	55.66	60.07	62.81	64.83	66.44	67.79	68.95	69.97	70.88	71.71
Biofuel	45.96	49.60	51.87	53.53	54.86	55.98	56.93	57.78	58.53	59.21
Ethanol	68.55	73.98	77.36	79.84	81.83	83.49	84.91	86.17	87.29	88.31
The average droplet size (Sauter mean size) [mm]										
Kerosene	0.039	0.028	0.023	0.020	0.018	0.016	0.015	0.014	0.013	0.013
Biofuel	0.052	0.037	0.030	0.027	0.024	0.022	0.020	0.019	0.018	0.017
Ethanol	0.029	0.021	0.017	0.015	0.013	0.012	0.011	0.010	0.010	0.009
Velocity [m/s]										
Kerosene	49.938	70.622	86.494	99.875	111.664	122.322	132.123	141.245	149.813	157.917
Biofuel	47.272	66.853	81.877	94.544	105.703	115.792	125.070	133.705	141.816	149.487
Ethanol	50.347	71.202	87.204	100.695	112.580	123.325	133.207	142.404	151.042	159.210

To better visualize the variation of key injector parameters as a function of pressure, the following graphs are plotted:

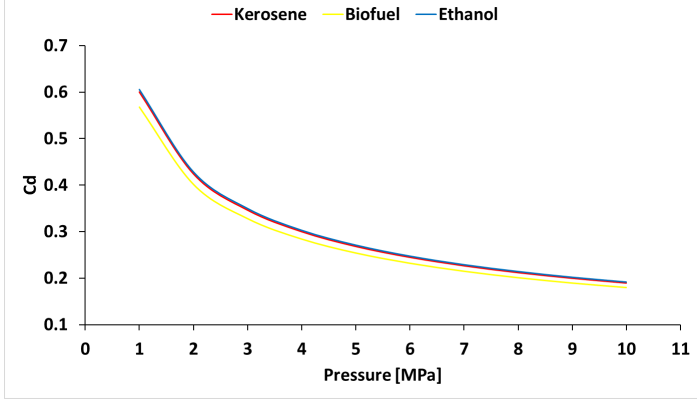

Figure 5. Variation of the discharge coefficient with respect to pressure

It can be observed that the discharge coefficient (Cd) decreases as the fluid pressure increases, and there are practically no significant differences between the values for kerosene and ethanol. However, there is a slight difference between kerosene and biofuel.

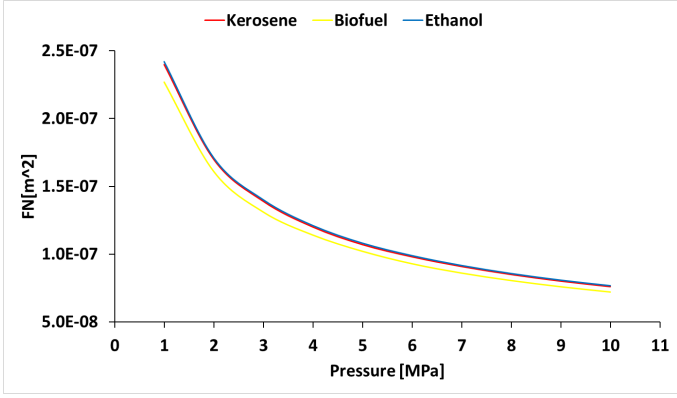

Figure 6. Variation of the flow rate number with respect to pressure

It can be observed that the flow rate number FN decreases as the fluid pressure increases, and there are practically no significant differences between the values for kerosene and ethanol. However, there is a slight difference between kerosene and biofuel.

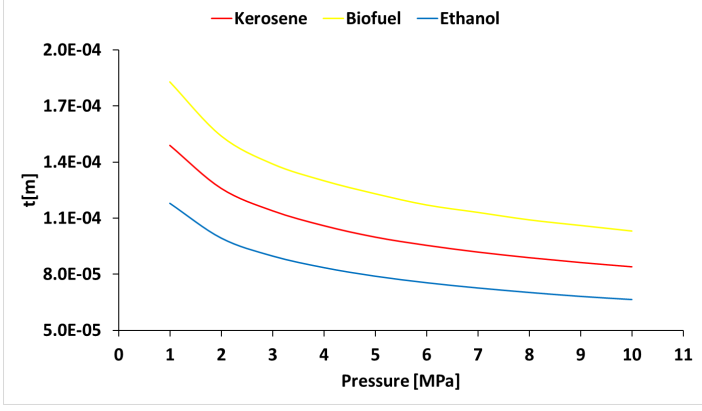

Figure 7. Variation of the film thickness with respect to pressure

It can be observed that the film thickness decreases as the fluid pressure increases, and there are significant differences between the values for kerosene, biofuel and ethanol. The film thickness for biofuel is higher than that for kerosene, while for ethanol, it is lower than that for kerosene.

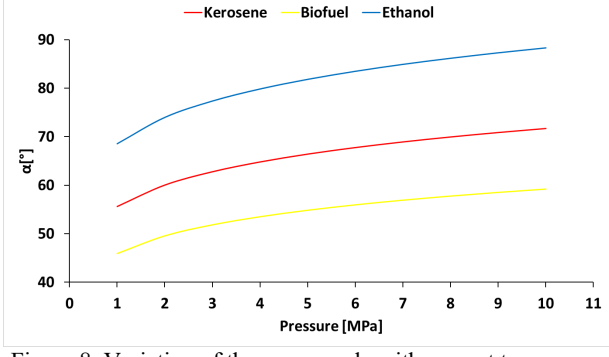

Figure 8. Variation of the spray angle with respect to pressure

It can be observed that the spray nozzle increases as the fluid pressure increases, and there are significant differences between the values for kerosene, biofuel and ethanol. The film spray nozzle for ethanol is higher than that for kerosene, while for biofuel, it is lower than that for kerosene.

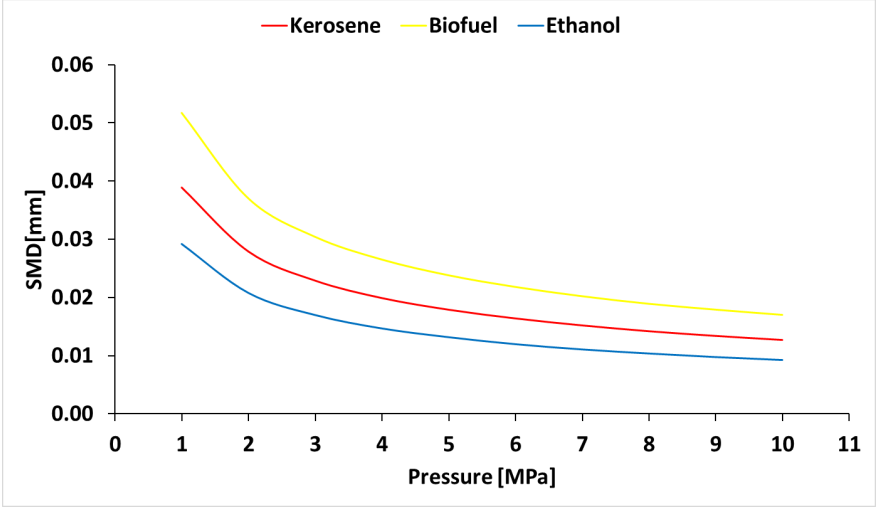

Figure 9. Variation of the average droplet with respect to pressure

It can be observed that the SMD decreases as the fluid pressure increases, and there are significant differences between the values for kerosene, biofuel and ethanol. The SMD for biofuel is higher than that for kerosene, while for ethanol, it is lower than that for kerosene.

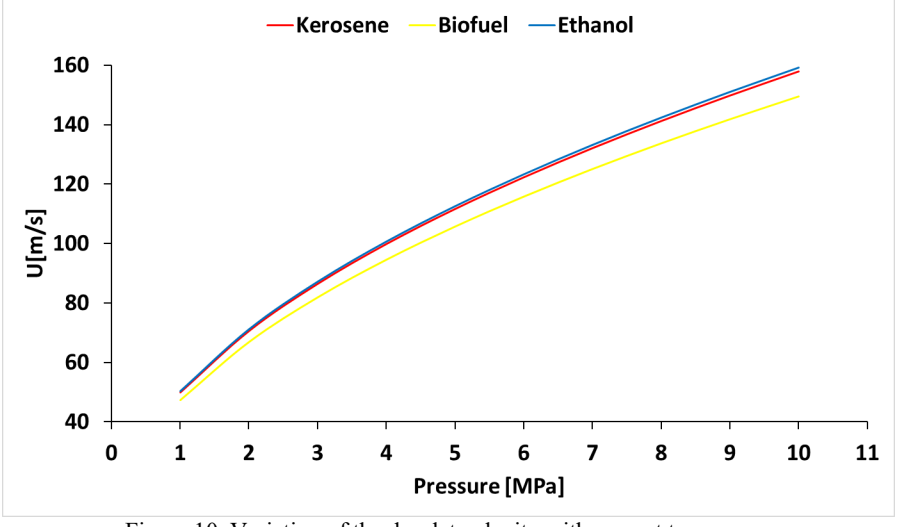

Figure 10. Variation of the droplet velocity with respect to pressure

It can be observed that the velocity increases as the fluid pressure increases, and there are not significant differences between the values for kerosene, biofuel and ethanol. The velocity for biofuel is lower than that kerosene and the ethanol and the difference increase as the fluid pressure increases.

3.2 Numerical simulation results

Numerical simulations were performed for 3 inlet pressures: 1, 5, and 10 MPa, using kerosene, biofuel and ethanol.

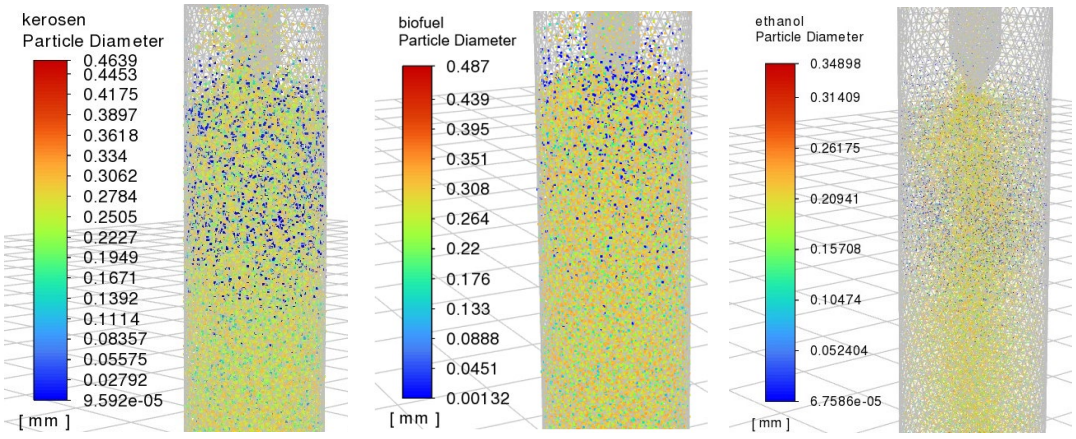

a) b) c)

Figure 11. The particle size for pentru $\Delta P = 1$ MPa, a) kerosene, b) biofuel, c) ethanol

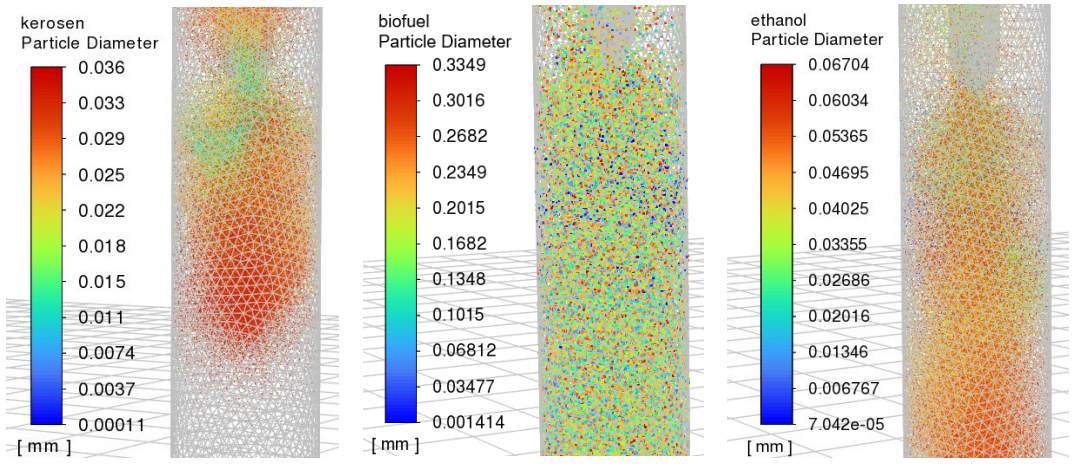

a) b) c)

Figure 12. The particle size for $\Delta P = 5$ MPa, a) kerosene, b) biofuel, c) ethanol

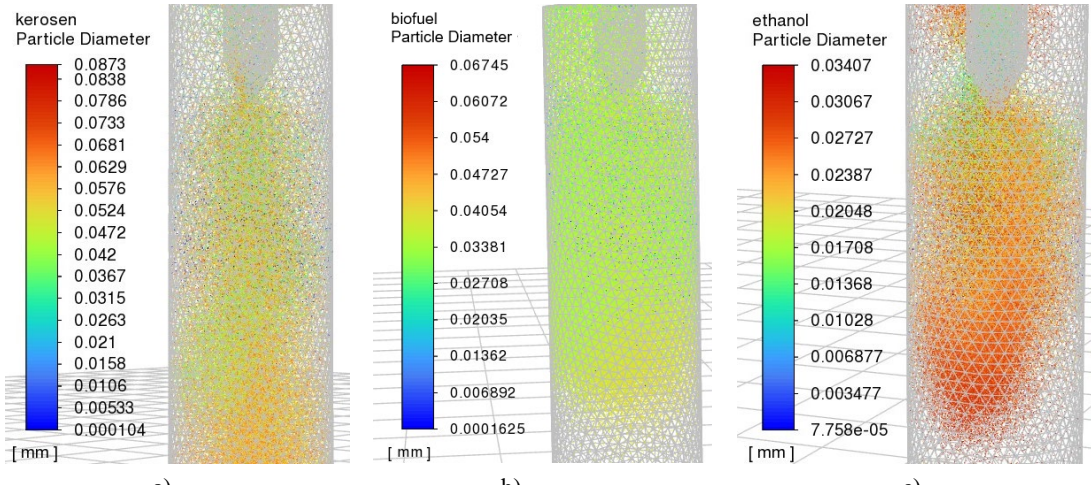

a) b) c)

Figure 13. The particle size for $\Delta P = 10$ MPa, a) kerosene, b) biofuel, c) ethanol

Furthermore, to verify the mathematical model, the images below depict particles with the dimensions obtained in the analytical calculation.

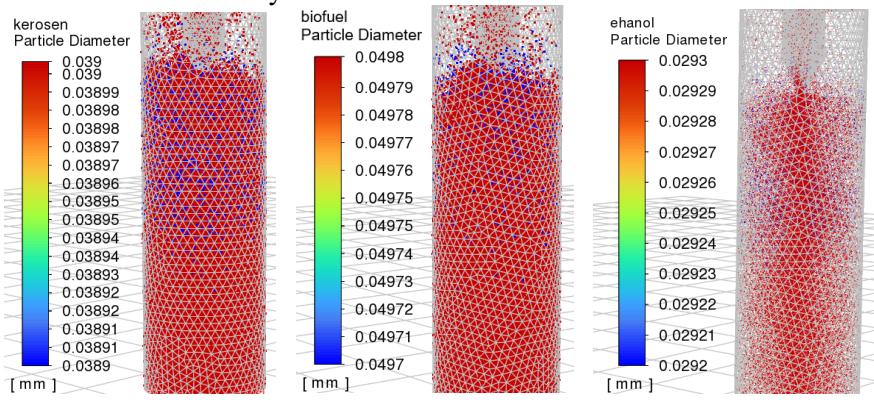

a) b) c)

Figure 14. The particle distribution with dimensions from the analytical model for $\Delta P = 1$ MPa, a) kerosene, b) biofuel, c) ethanol

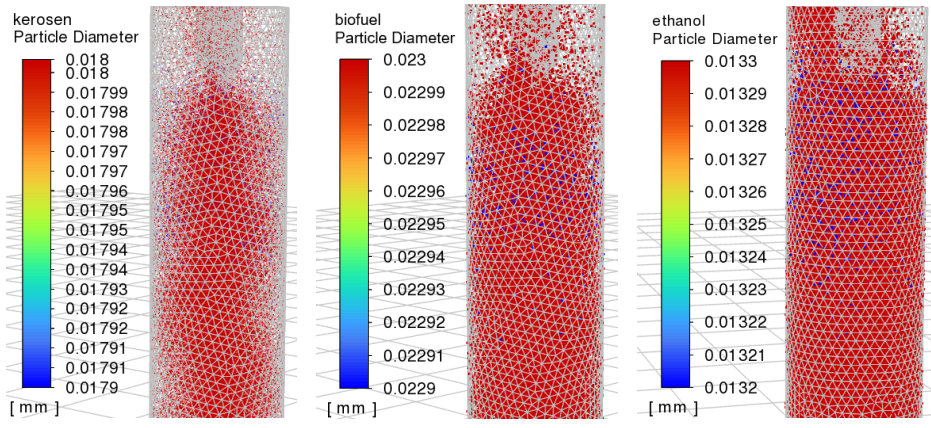

a) b) c)

Figure 15. The particle distribution with dimensions from the analytical model for $\Delta P = 5$ MPa, a) kerosene, b) biofuel, c) ethanol

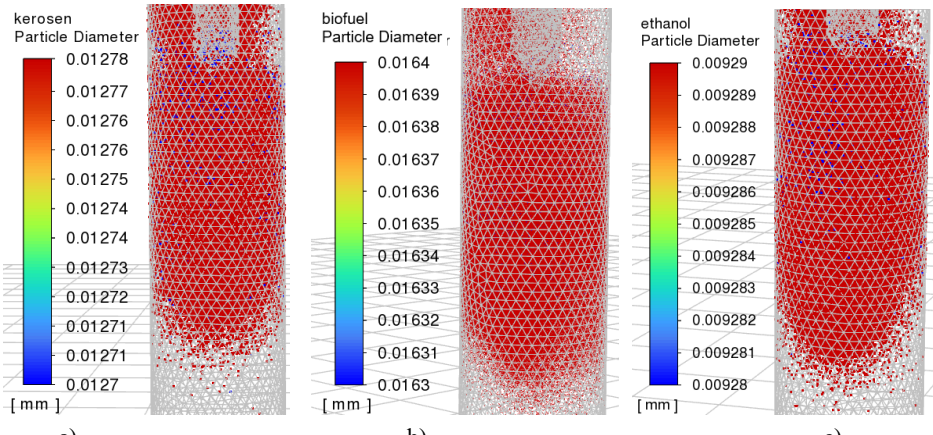

a) b) c)

Figure 16. The particle distribution with dimensions from the analytical model for $\Delta P = 10$ MPa, a) kerosene, b) biofuel, c) ethanol

Next, the current lines inside the simulation domain are presented.

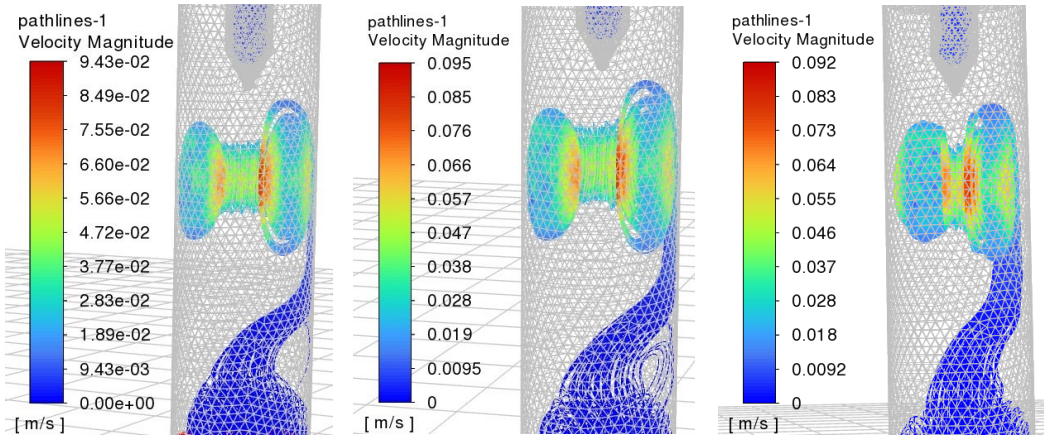

a) b) c)

Figure 17. The streamlines for $\Delta P = 1$ MPa, a) kerosene, b) ethanol, c) biofuel

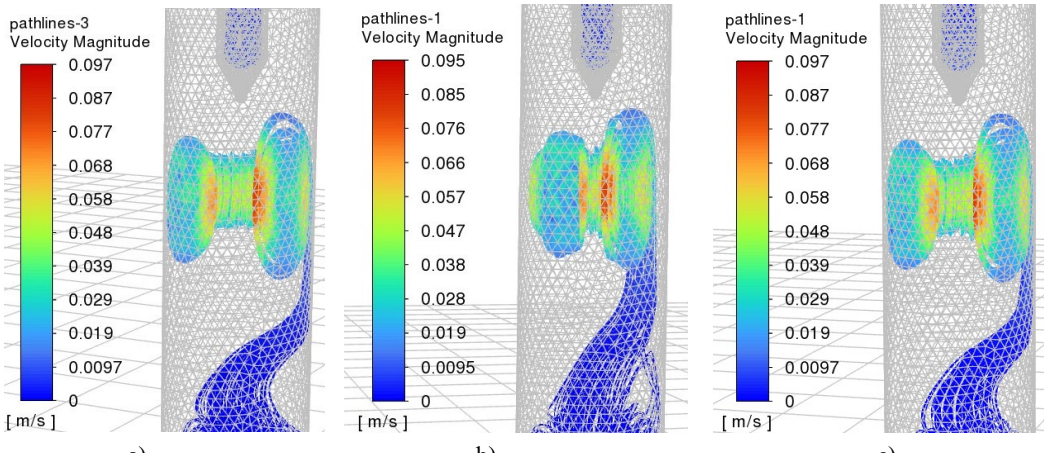

a) b) c)

Figure 18. The streamlines for $\Delta P = 5$ MPa, a) kerosene, b) ethanol, c) biofuel

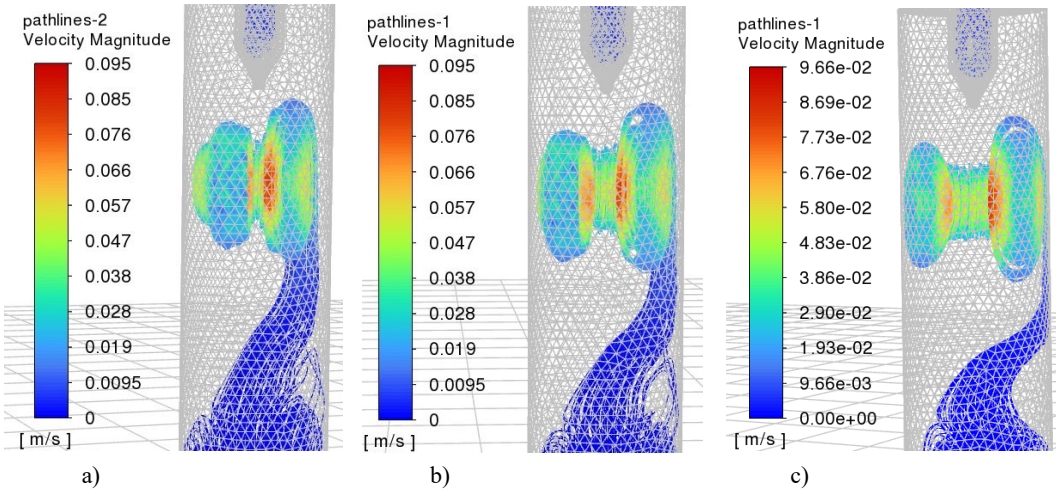

a) b) c)

Figure 19. The streamlines for $\Delta P = 10$ MPa, a) kerosene, b) ethanol, c) biofuel

Analyzing the results obtained from the simulation, it can be observed that the average droplet size, calculated as a result, falls within the range of the results obtained from the simulation.

4. CONCLUSIONS

In this study, an analysis of the characteristics defining the effective atomization of fuel was conducted. Three fuels were analyzed, namely kerosene, ethanol, and biofuel, which were sprayed using a simplex-type injector.

In the case of the proposed injector, specifically a simplex-type injector with a swirl chamber represented by a pintle, the most optimal fuel among the three liquids studied is ethanol. Ethanol has low viscosity and low density, which means that this type of fuel is easier to atomize with our injector compared to pure biofuel, which has higher density and viscosity values. Calculations revealed the qualities that ethanol exhibits after atomization, specifically a thin liquid film thickness, a wide spray angle consisting of small droplets, at any pressure difference compared to the other fuels studied.

In terms of the flow number, ethanol and kerosene are the most suitable liquids for atomization at high pressures. It was observed that the pressure difference has a significant influence on liquid atomization. The best atomization qualities and optimal values were obtained when the pressure difference was high. An example can be seen in the calculations, where it is evident that the smallest average droplet sizes occur when the pressure difference is high, and this trend holds for other characteristics as well.

For the injector used in the calculations, kerosene can also be used, as it exhibits average atomization properties. The obtained values are not as satisfying as those of ethanol but are also not as unsatisfactory as those of pure biofuel.

From the simulations performed, it can be observed that the empirical formulas used to determine average droplet sizes have good accuracy. The values obtained using these formulas consistently fell within the ranges of results obtained from the simulations. Since the Sauter Mean Diameter (SMD) depends on both half of the spray angle and the film thickness, it can be concluded that all empirical formulas used in the calculations have satisfactory precision.

In conclusion, for a pressure difference equal to 1.00E+07 Pa, atomization is significantly better, resulting in smaller fuel particle sizes. As evident from the simulations, atomization has an optimal shape when there are large pressure differences.

REFERENCES

[1] R. A. Dafsari, H. J. Lee, J. Han, J. Lee, Evaluation of the atomization characteristics of aviation fuels with different viscosities using a pressure swirl atomizer, *International Journal of Heat and Mass Transfe*r, Vol **145**, 118704, https://doi.org/10.1016/j.ijheatmasstransfer.2019.118704, 2019.

[2] V. Aslan, Fuel characterization, engine performance characteristics and emissions analysis of different mustard seed biodiesel: An overview, *Journal of Biotechnology*, Volume **37**0, Pages 12-30, https://doi.org/10.1016/j.jbiotec.2023.05.006, 2023.

[3] G. Cican, M. Deaconu, R. Mirea, L. C. Ceatra, M. Cretu, An Experimental Investigation to Use the Biodiesel Resulting from Recycled Sunflower Oil, and Sunflower Oil with Palm Oil as Fuels for Aviation Turbo-Engines, *Int. J. Environ. Res. Public Health*, **18**, 5189. https:// doi.org/10.3390/ijerph18105189, 2021.

[4] G. Cican, D. E. Crunteanu, R. Mirea, L. C. Ceatra, C. Leventiu, Biodiesel from Recycled Sunflower and Palm Oil - A Sustainable Fuel for Microturbo-Engines Used in Airside Applications, *Sustainability* 2023, **15**, 2079. https://doi.org/10.3390/su15032079

[5] R. Przysowa, B. Gawron, T. Białecki, A. Ł ¸egowik, J. Merkisz, R. Jasi ´nski, Performance and Emissions of a Microturbine and Turbofan Powered by Alternative Fuels, *Aerospace* 2021, **8**, 25, https://doi.org/10.3390/ aerospace8020025
[6] Z. Tian, X. Zhen, Y. Wang, D. Liu, X. Li, Comparative study on combustion and emission characteristics of methanol, ethanol and butanol fuel in TISI engine, *Fuel* 2020, 259. [CrossRef]
[7] A. Elfasakhany, State of Art of Using Biofuels in Spark Ignition Engines, *Energies* 2021, **1**4, 779. https://doi.org/10.3390/en14030779
[8] S. Osman, O. V. Sapunaru, A. E. Sterpu, T. V. Chis, C. I. Koncsag, Impact of Adding Bioethanol and Dimethyl Carbonate on Gasoline Properties, *Energies* 2023, **16**, 1940. https://doi.org/10.3390/en16041940
[9] G. Cican, M. Deaconu, R. Mirea, A. T. Cucuruz, Influence of Bioethanol Blends on Performances of a Micro Turbojet Engine, *Rev. Chim.*, **71**(5), 2020, 229-238. https://doi.org/10.37358/RC.20.5.8131
[10] L. Chen, Z. Zhang, Y. Lu, C. Zhang, X. Zhang, C. Zhang, A. P. Roskilly, Experimental study of the gaseous and particulate matter emissions from a gas turbine combustor burning butyl butyrate and ethanol blends, *Appl. Energy* 2017, **195**, 693–701. [CrossRef]
[11] H. M. Gad, E. A. Baraya, T. M. Farag, I. A. Ibrahim, Effect of geometric parameters on spray characteristics of air assisted pressure swirl atomizer, *Alexandria Engineering Journal*, Volume **61**, Issue 7, 2022, Pages 5557-5571, https://doi.org/10.1016/j.aej.2021.11.010.
[12] J. Chen, J. Li, and L. Yuan, Effects of inlet pressure on ignition of spray combustion, *International Journal of Aerospace Engineering*, vol. **2018**, Article ID 3847264, 13 pages, 2018.
[13] L. Song, T. Liu, W. Fu, and Q. Lin, Experimental study on spray characteristics of ethanol-aviation kerosene blended fuel with a high-pressure common rail injection system, *Journal of the Energy Institute*, vol. **91**, no. 2, pp. 203–213, 2016.
[14] M. Kumar, S. Karmakar, S. Kumar and S. Basu, Experimental investigation on spray characteristics of Jet A-1 and alternative aviation fuels, *International Journal of Spray and Combustion Dynamics*, **202**, DOI: 10.1177/17568277211010140
[15] U. Kesieme, K. Pazouki, A. Murphy, et al., Biofuel as an alternative shipping fuel: technological, environmental and economic assessment, *Sustainable Energy Fuels* 2019, **3**: 899–909.
[16] R. N. A. Francis, *Investigation of Fuel Nozzle Technologies to Reduce Gas Turbine missions*, 2015
[17] T. Zhang, B. Dong, X. Zhou, L. Guan, W. Li, and S. Zhou, Experimental Study of Spray Characteristics of Kerosene-Ethanol, *International Journal of Aerospace Engineering*, Volume **2018**, https://doi.org/10.1155/2018/2894908
[18] L. Bayvel, Z. Orzechowski, *Liquid Atomization*, Taylor & Francis, 1993, pp. 132, 172.